Entropy **2014**, *16*, 5560-5574; doi:10.3390/e16105560

OPEN ACCESS

entropy

ISSN 1099-4300

www.mdpi.com/journal/entropy

Article

Contributions to the Transformation Entropy Change and Influencing Factors in Metamagnetic Ni-Co-Mn-Ga Shape Memory Alloys

Concepció Seguí * and Eduard Cesari

Departament de Física, Universitat de les Illes Balears, Campus universitari, Ctra. de Valldemossa km 7.5, 07122 Palma de Mallorca, Spain; E-Mail: eduard.cesari@uib.cat

* Author to whom correspondence should be addressed; E-Mail: concepcio.segui@uib.es; Tel.: +34-971-173224; fax: +34-971-173426.

External Editor: Lluís Mañosa

Received: 17 September 2014; in revised form: 15 October 2014 / Accepted: 16 October 2014 / Published: 22 October 2014

Abstract: Ni-Co-Mn-Ga ferromagnetic shape memory alloys show metamagnetic transition from ferromagnetic austenite to paramagnetic (or weak-magnetic) martensite for a limited range of Co contents. The temperatures of the structural and magnetic transitions depend strongly on composition and atomic order degree, in such a way that combined composition and thermal treatment allows obtaining martensitic transformation (MT) between any magnetic state of austenite and martensite. The entropy change ΔS measured in the magnetostructural transition comprises a magnetic contribution which depends on the type and degree of magnetic order of the related phases. Consequently, both the magnetization jump across the MT (ΔM) and ΔS are composition and atomic order dependent. Both ΔS and ΔM determine the effect of applied magnetic fields on the MT, hence knowledge and understanding of their behavior can help to approach the best conditions for magnetic field induced MT and related effects. In previous papers, we have reported findings regarding the behavior of the transformation entropy in relation to composition and atomic order in $Ni_{50-x}Co_xMn_{25+y}Ga_{25-y}$ (x = 3–8, y = 5–7) alloys. In the present paper we will review our recent results, summarizing the key findings and drawing general conclusions regarding the magnetic contribution to ΔS and the effect of different factors on the magnetic and structural properties of these metamagnetic alloys.

Keywords: Ni-Co-Mn-Ga; transformation entropy change; atomic order; metamagnetic shape memory alloys

PACS Codes: 64.70.Kd; 75.30.Kz; 81.30.Kf

1. Introduction

The Heusler Ni-Mn-X (X = In, Sn, Sb) *metamagnetic* shape memory alloys (MSMAs) have attracted much attention since the discovery of magnetic field-induced reverse martensitic transformation in Ni-Mn-In [1]. On cooling, these alloys undergo martensitic transformation (MT) from the ordered $L2_1$ structure to low magnetization martensite [2–5], which is accompanied by a large magnetization drop (ΔM). The occurrence of such magnetostructural transition opens the possibility for magnetic shape memory effect (MSM) [2], and other properties resulting from the interaction between the structural and magnetic transitions, such as giant magnetoresistance and magnetocaloric effect [6,7]. Doping of the above alloys with Co [2,8,9] has been found to enhance the ferromagnetic character of austenite enlarging the magnetization difference across the MT.

For the well-known close to stoichiometric Ni_2MnGa alloys, both austenite and martensite display ferromagnetic properties, and therefore ΔM is usually very small [10], preventing the occurrence of magnetic field induced MTs. However, Co addition in this case not only increases the ferromagnetic coupling of austenite but also weakens the magnetic interactions of martensite through partial antiferromagnetic coupling [3,9]; thus, *metamagnetic* transition from ferromagnetic austenite (*A*) to paramagnetic (or weak-magnetic) martensite (*m*) may occur, accompanied by significant magnetization change [11–15].

Owing to the composition dependence of the MT and Curie temperatures—both in austenite and martensitic phases- metamagnetic transition occurs for a limited range of Co contents [12,14]. In this sense, the composition-temperature phase diagram for $Ni_{50-x}Co_xMn_{25+y}Ga_{25-y}$ (x = 3–8, y = 5–7) alloys [15] shows that the $A_{ferro} \leftrightarrow m_{para}$ MT occurs for electron to atom ratio (*e/a*) between 7.58 and 7.67, being $A_{para} \leftrightarrow m_{para}$ above and $A_{ferro} \leftrightarrow m_{ferro}$ below this range. In conclusion, for the proper composition range, Ni-Co-Mn-Ga alloys are metamagnetic; indeed, magnetic field induction of the MT has been recently found in such alloys [16,17].

Along with composition, another crucial factor in determining the MT characteristics and magnetic properties of Heusler alloys is atomic order [18–20]. The atomic order degree of the $L2_1$ austenite can be modified by means of thermal treatments: atomic disorder can be forced by quench from temperatures around the $B2 \leftrightarrow L2_1$ transition, and progressive ordering occurs by ageing at temperatures at which atomic diffusion is possible, as proven by neutron diffraction experiments in several Ni-Mn-based alloys [18,21,22].

For the above mentioned Ni-Co-Mn-Ga alloys, it has been found that the austenite and martensite Curie temperatures (T_C^A , T_C^m respectively), increase as atomic order degree does, whereas the martensitic transformation temperatures (forward M_p and reverse A_p) tend to decrease. Such opposite changes make that, for a given composition, the transformation sequence on cooling/heating depends

on the atomic order; for example, poorly ordered alloys with high *e/a* display the $A_{para}\leftrightarrow m_{para}\leftrightarrow m_{ferro}$ sequence, evolving to $A_{para}\leftrightarrow A_{ferro}\leftrightarrow m_{para}\leftrightarrow m_{ferro}$ as ordering improves, while for low *e/a* alloys the transformation sequence changes from $A_{para}\leftrightarrow A_{ferro}\leftrightarrow m_{para}\leftrightarrow m_{ferro}$ to $A_{para}\leftrightarrow A_{ferro}\leftrightarrow m_{ferro}$. Consequently, combined composition and thermal treatment allows obtaining MT between any magnetic state of austenite and martensite [23].

It is worth noting that the evolution of MT temperatures with atomic ordering shows stages related to different magnetic exchanges, *i.e.*, $A_{para}\leftrightarrow m_{para}$, $A_{ferro}\leftrightarrow m_{para}$ or $A_{ferro}\leftrightarrow m_{ferro}$ [23]. To explain such behavior, which is a clear demonstration of the mutual influence between magnetic and atomic order, it is suggested that ordering brings about magnetization-dependent free energy drops which modify the relative stability of the phases [21,23].

The entropy change ΔS measured in the magnetostructural transition comprises structural and magnetic contributions, the latter depending on the type and degree of magnetic order of the related phases. Of course it means that ΔS changes from one transformation sequence to another, but it also includes a more specific dependence on ($T_C^A - To$) (To is the equilibrium temperature of the MT). While a decrease of ΔS with increasing ($T_C^A - To$) has been widely proven for different metamagnetic alloys [14,15,24–26], a phenomenological model has been recently developed, based on a Bragg–Williams approximation, accounting for the magnetic contribution. The model achieves excellent agreement between calculated and experimental ΔS for different composition and atomic order degrees, corroborating the magnetic origin of changes in transformation entropy [23,27].

According to the Clausius-Clapeyron relationship:

$$\frac{dT}{dH} = -\mu_0 \frac{\Delta M}{\Delta S} \tag{1}$$

both ΔS and ΔM are essential contributions to the transformation temperature shift due to applied magnetic field. Therefore, knowledge and understanding of the dependence of ΔS on composition and atomic ordering can help to approach the best conditions for magnetic field induced MT and related effects.

In previous papers, we have reported findings regarding the behavior of the transformation entropy in relation to composition and atomic order in the Ni-Co-Mn-Ga alloy system; we have been able to evaluate the magnetic contribution to ΔS and we have made progress in understanding the effects of different factors on the magnetic and structural properties of the metamagnetic alloys. In the present work, we will basically review our recent results, summarizing the key findings and drawing general conclusions.

2. Experimental Procedures

The results on which this article is based were obtained for a set of polycrystalline $Ni_{50-x}Co_xMn_{25+y}Ga_{25-y}$ (x = 3–8, y = 5–7) alloys, prepared by arc melting in Ar atmosphere, from high purity elemental metals. The ingots were homogenized in vacuum quartz ampoules at 1170 K for 24 h. The actual composition of the homogenized alloys was determined by energy-dispersive X-ray spectroscopy (EDS, Bruker X-flash detector 4010, Bruker GmbH, Berlin, Germany) in a scanning electron microscope (Hitachi S-3400 N, Hitachi High-Tech Ltd., Tokyo, Japan) and is given in Table 1.

Thermal treatments aimed to retain different degree of atomic order in the samples consisted of water quench from T_Q = 770–1170 K and post-quench ageing at T_A = 470–620 K.

The martensitic and magnetic transitions were monitored by thermogravimetric analysis (TGA, TA SDT Q600, TA Instruments, New Castle, DE, USA) performed under the influence of a permanent magnet, see [14,15] for details. Although the used TGA system provides simultaneous measurement of weight change and differential heat flow on the same sample, additional differential scanning calorimeter (TA DSC 2920) measurements were performed whenever required. The MT and austenite/martensite Curie temperatures are obtained from TGA/DSC curves, and the transformation entropy changes for the forward ($A \rightarrow m$) and reverse ($m \rightarrow A$) MTs are determined from the calorimetric peaks as $\Delta S^{A \rightarrow m} = Q^{A \rightarrow m}/M_p$ and $\Delta S^{m \rightarrow A} = Q^{m \rightarrow A}/A_p$, ($Q^{A \rightarrow m}$, M_p and $Q^{m \rightarrow A}$, A_p, are the corresponding transformation heats and peak temperatures). The entropy changes calculated in this way do not differ significantly from those obtained integrating $\delta Q/T$ over the complete transformation ranges, and are accurate enough if it is further considered that the shape of the calorimetric peaks is quite the same for all studied cases.

Table 1. Nominal and determined compositions (at.%) for the studied alloys.

Al.#	Nominal Composition	Ni	Co	Mn	Ga	e/a
C1	$Ni_{42}Co_8Mn_{32}Ga_{18}$	41.6	7.9	32.4	18.1	7.68
C2	$Ni_{43}Co_7Mn_{30}Ga_{20}$	43.2	7.4	29.6	19.8	7.65
C3	$Ni_{43.5}Co_{6.5}Mn_{31}Ga_{19}$	42.7	6.1	31.5	19.8	7.61
C4	$Ni_{43.5}Co_{6.5}Mn_{30}Ga_{20}$	42.7	6.5	30.1	20.8	7.58
C5	$Ni_{45}Co_5Mn_{31}Ga_{19}$	44.8	2.8	31.4	21.0	7.56

3. Results and Discussion

3.1. Composition and Atomic Order Effects on the Magnetic and Structural Transformations

To illustrate how composition and atomic order affect the magnetic and structural transformations in the studied alloys, Figure 1 shows the TGA and DSC curves obtained for alloys C2 (a) and C4 (b) just after water quench from 970 K and after long post-quench ageing (7 days) at 470 K.

As it can be seen in Figure 1, quenched—thus poorly ordered- alloy C2, displays $A_{para} \leftrightarrow m_{para}$ MT, evolving to $A_{ferro} \leftrightarrow m_{para}$ as ordering improves, while for alloy C4 the MT changes from $A_{ferro} \leftrightarrow m_{para}$ to $A_{ferro} \leftrightarrow m_{ferro}$. Transferring the MT temperatures (M_p, A_p) and the austenite and martensite Curie temperatures (T_C^A, T_C^m) for quenched and aged alloys C1 to C5 to a transformation temperatures *vs.* electron to atom ratio (*e/a*), the phase diagram shown in Figure 2 is obtained. It can be seen that the *e/a* domain for metamagnetic behaviour shifts from 7.55–7.63 immediately after water quench from 1070 K to 7.61–7.69 after prolonged ageing.

The evolution of the transformation temperatures with atomic ordering can be seen in more detail if they are plotted as a function of ageing time after water quench, as shown in Figure 3 for alloys C2 (a) and C4 (b). The relative position of the structural and magnetic transitions indicates the occurrence of a given transformation sequence. It is worth noting that, while the Curie temperatures increase

monotonically with ageing time, the evolution of MT temperatures shows stages related to different magnetic exchanges.

Figure 1. TGA (left axis) and DSC curves (right axis) obtained for alloy C2 (a) and C4 (b) just after water quench from 970 K (dashed lines) and after 7 days post-quench ageing at 470 K (solid lines). Representative temperatures for the martensitic and magnetic transitions are indicated (adapted from [23]).

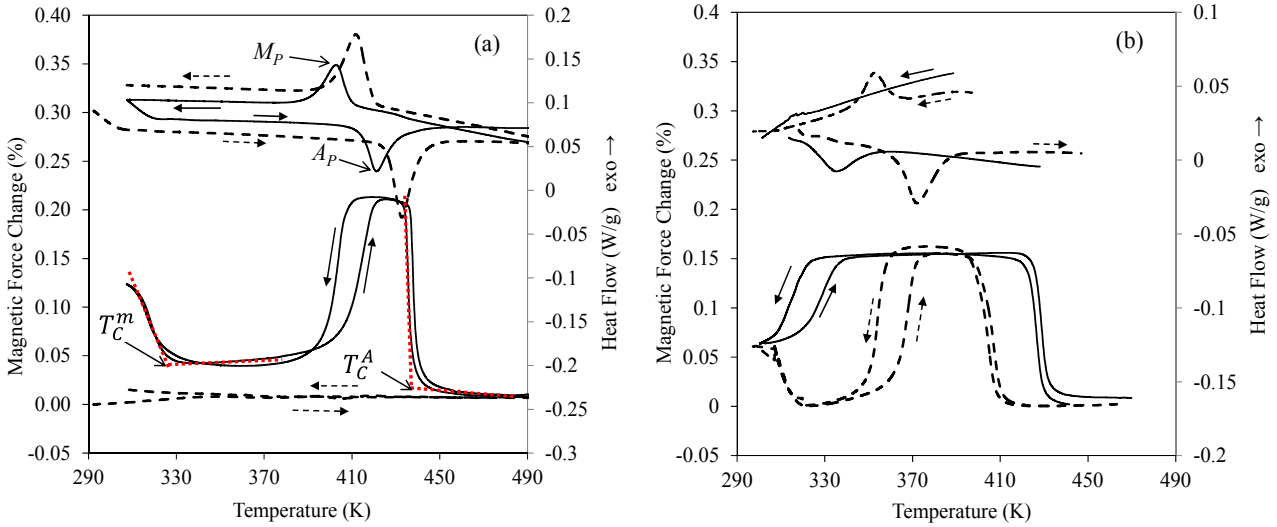

Figure 2. Dependence of the structural and magnetic transformation temperatures (▲ T_C^A ,◇A_P, ◆ M_P and □ T_C^m) on the electron to atom ratio, (**a**) after water quench from 1070 K and (**b**) after 100 min aging at 520 K. Crosses are used for extrapolated T_C^A values (adapted from [15]).

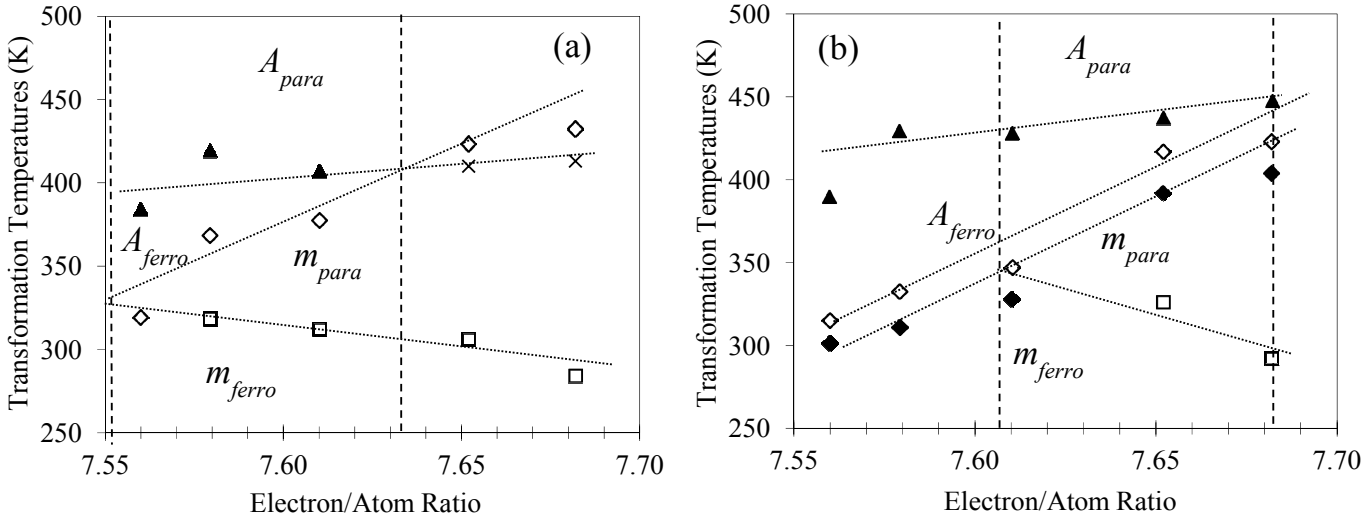

Figure 3. Evolution of the transformation temperatures (○ T_C^A , ● A_p, ◆ M_p and ● T_C^m) with ageing time at 470 K (after water quench from 970 K) for alloys C2 (a) and C4 (b). For $T_C^A < M_p$ (alloy C2) and $T_C^m > A_p$ (alloy C4) Curie temperatures are extrapolated and indicated as × (adapted from [15]).

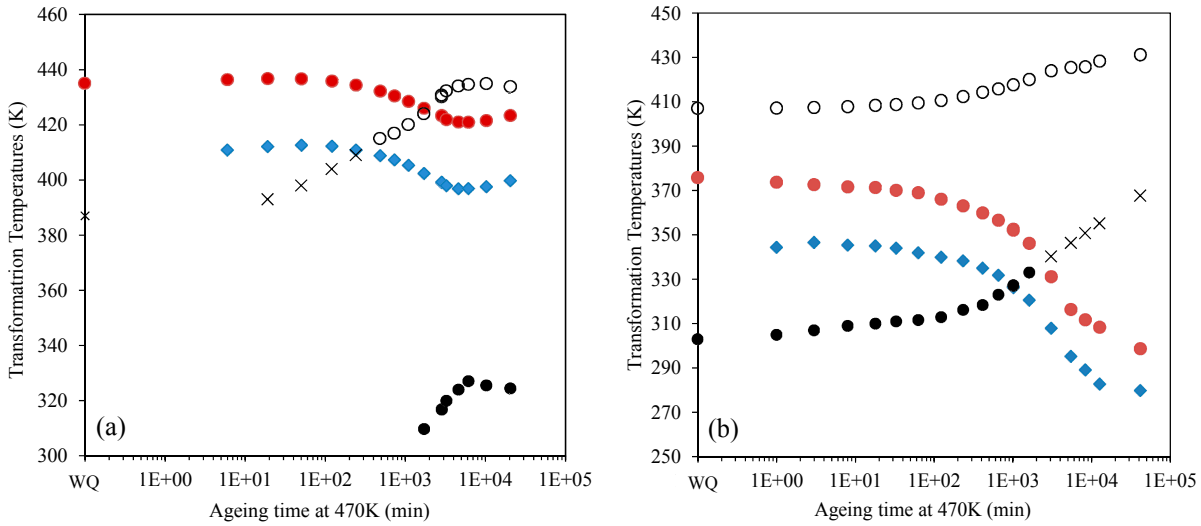

Such behavior is a clear demonstration of the mutual influence between magnetic and atomic order, and it has been suggested that atomic ordering brings about magnetization-dependent free energy drops, which modify the relative stability of the phases [21,23].

3.2. Contributions to the Entropy Change at the Magnetostructural Transformation

The main contributions to the measured transformation entropy changes, as commonly accepted, include structural and magnetic contributions [14,26]:

$$\Delta S^{A\to m} = \Delta S_{strc}^{A\to m} + \Delta S_{mag}^{A\to m} - \tag{2}$$

$$\Delta S^{m\to A} = \Delta S_{strc}^{m\to A} + \Delta S_{mag}^{m\to A} \tag{3}$$

where $\Delta S_{strc}^{A\to m} < 0$ and $\Delta S_{strc}^{m\to A} = \left|\Delta S_{strc}^{A\to m}\right| > 0$, since the lattice vibration entropy of the cubic austenite is larger than that of the *m* phase, with a more close packed structure. Instead, the sign and value of $\Delta S_{mag}^{A\to m}$, $\Delta S_{mag}^{m\to A}$ depend on the magnetic exchange interaction between the related phases. A possible magnetostructural coupling term is here disregarded.

It can be expected that $\Delta S_{mag}^{A\to m} = 0$ if neither austenite nor martensite exhibit magnetic order, as in a $A_{para}\leftrightarrow m_{para}$ transformation; instead, $\Delta S_{mag}^{A\to m} > 0$ (and $\Delta S_{mag}^{m\to A} < 0$) if the magnetization decreases upon the ($A\to m$) transformation, as in a $A_{ferro}\leftrightarrow m_{para}$ MT. For $A_{ferro}\leftrightarrow m_{ferro}$, $\Delta S_{mag}^{A\to m}$ can be either positive or negative depending on the relative value of magnetization of austenite and martensite. For metamagnetic MTs, the absolute values of the transformation entropy changes are then:

$$\left|\Delta S^{A\to m}\right| = \left|\Delta S_{strc}^{A\to m}\right| - \left|\Delta S_{mag}^{A\to m}\right| \tag{4}$$

$$\left|\Delta S^{m\to A}\right| = \left|\Delta S_{strc}^{m\to A}\right| - \left|\Delta S_{mag}^{m\to A}\right| \tag{5}$$

and since magnetic order of austenite improves as temperature drops below Curie temperature, the greater the temperature gaps (T_C^A -M_p) or (T_C^A -A_p), the greater the magnetic contribution to the entropy change, hence the overall transformation entropy diminishes, as it has been observed for many different metamagnetic alloys [14,15,24–26]. Owing to the thermal hysteresis of the MT, (T_C^A -M_p) > (T_C^A -A_p), so in general $\left|\Delta S_{mag}^{A\to m}\right| > \left|\Delta S_{mag}^{m\to A}\right|$ leading to measured $|\Delta S^{A\to m}| < |\Delta S^{m\to A}|$. This fact, and its relationship with the relative position of the MT and T_C^A, was analyzed for alloy C1 in a previous work [14], and can be summarized as shown in Figure 4, where $|\Delta S^{A\to m}|$ and $|\Delta S^{m\to A}|$, together with (T_C^A –T_O) (T_O = ½(M_p + A_p)), are represented against ageing time after water quench from 1070 K. As the temperature gap increases with ageing time –that is, as atomic order improves-, the overall transformation entropy decreases, until getting stabilized for long ageing time; in the metamagnetic region it holds that $|\Delta S^{A\to m}| < |\Delta S^{m\to A}|$, but for $T_C^A < T_O$, where the $A_{para}\leftrightarrow m_{para}$ MT occurs, it is observed that $|\Delta S^{A\to m}| > |\Delta S^{m\to A}|$, which can only be fulfilled if "paramagnetic" martensite has higher degree of magnetic order than paramagnetic austenite [14]. Among other reasons, it could be due to antiferromagnetic rather than paramagnetic behavior of martensite, as suggested for the metamagnetic Ni-Mn-In, Ni-Co-Mn-In or Ni-Co-Mn-Sn [2,4,8,10], and also for Co-doped Ni-Mn-Ga [28], although there is still a lack of knowledge on this point.

Figure 4. Transformation entropy changes (absolute values) measured for the forward (□ $|\Delta S^{A\to m}|$) and reverse (■ $|\Delta S^{m\to A}|$) MTs, and temperature gap (T_C^A –T_O) (●, right axis; open circles are used for extrapolated Curie temperatures), of alloy C1 as a function of ageing time at 570 K after WQ from 1070 K.

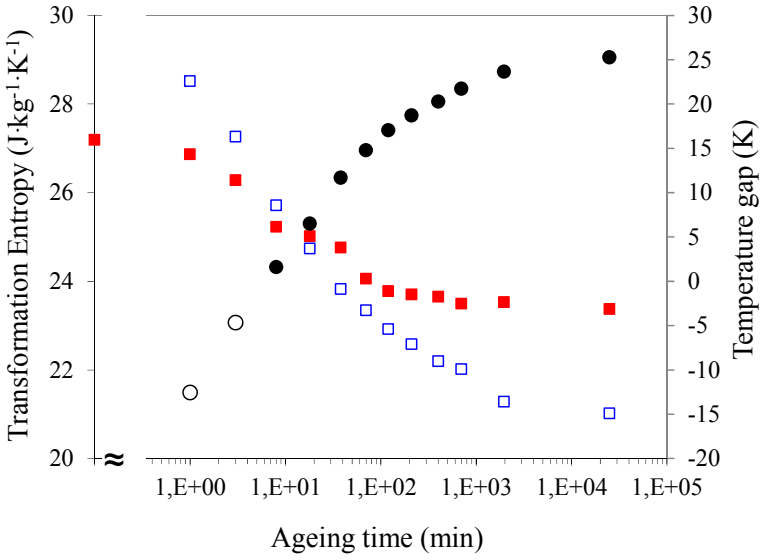

Regarding the magnetic properties of austenite and martensite, it is worth to mention that neutron scattering experiments have shown that improvement of atomic order increases the stability domain of ferromagnetic austenite (T_C^A increases) [18]. Moreover, strong effects of the order degree on the magnetization of both austenite and martensite have been observed in several metamagnetic alloys [29]. Therefore, aside from the effects of atomic order reported in this paper, variation of the order degree brings about changes in the dependence of ΔS and ΔM on the applied field, as it has been reported in [30].

Once the inequality of the entropy change for the forward and reverse transformations has been understood, in order to focus on other factors influencing the transformation entropy change, the average, absolute values, of the contributions to ΔS will be considered hereafter. In this way, a unique expression can be used:

$$\Delta S = \Delta S_{strc} - \Delta S_{mag} \quad (6)$$

3.3. Composition Dependence of the Transformation Entropy

Figure 5 shows the absolute values of the transformation entropy changes as a function of composition, for quenched –disordered- and long-aged –ordered- condition. The changes in transformation sequences brought about by ordering (see Figure 2) are indicated in Figure 5; unless otherwise specified, MT is $A_{ferro} \leftrightarrow m_{para}$. Composition dependence—and even atomic order dependence—of the structural contribution to the transformation entropy cannot be disregarded; indeed, for the two alloys with highest *e/a*, quenched, $\Delta S_{mag}=0$ is expected since they undergo the $A_{para} \leftrightarrow m_{para}$ MT, but nevertheless the measured entropy change differs from each other. However, we will consider that transformation entropy changes are mainly due to changes in the magnetic contribution.

Figure 5. Average absolute values of the transformation entropy changes as a function of the electron to atom ratio (*e/a*), after water quench from 1070 K (◊), and after 100 min aging at 520 K (◆). Unless otherwise specified, MT is $A_{ferro} \leftrightarrow m_{para}$.

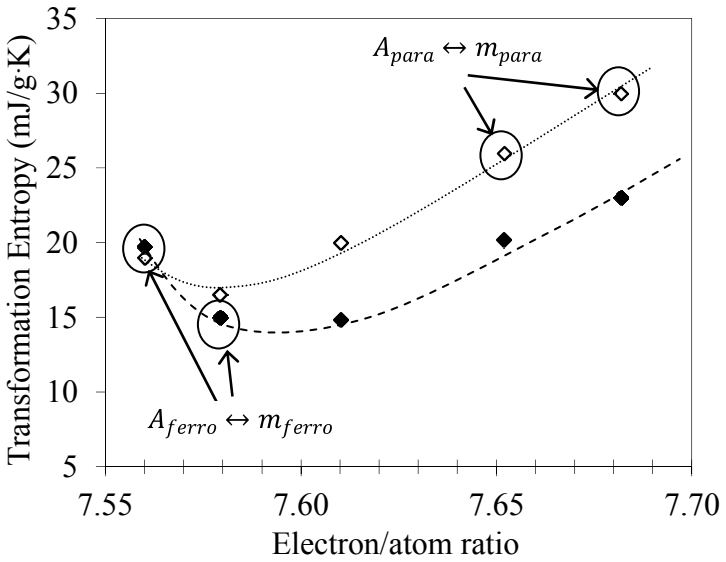

Paying attention to the aged condition, the transformation entropy is observed to increase towards higher *e/a* values, for which the temperature gap ($T_C^A - To$) decreases; this is indicative of progressive worsening of the magnetic order of austenite at the MT temperatures, which results in lowering of the magnetic contribution to the transformation entropy and hence the overall entropy increases. For low *e/a*, the MT changes from $A_{ferro} \leftrightarrow m_{para}$ to $A_{ferro} \leftrightarrow m_{ferro}$ for which the magnetization jump across the MT is smaller, the corresponding magnetic entropy decreases and thus the (absolute value) overall transformation entropy increases [15].

In any case, the magnetic contribution to the transformation entropy is the highest for the *e/a* values for which the MT switches from $A_{ferro}\leftrightarrow m_{para}$ to $A_{ferro}\leftrightarrow m_{ferro}$, where the largest possible ($T_C^A - T_O$) gap (maximum ΔS_{mag}) gives way to a decrease triggered by the increasingly ferromagnetic martensite.

3.4. Atomic Order Dependence of the Transformation Entropy

Owing to the effect of the magnetic order of the phases on the entropy change, and to the change of transformation sequence experienced by the alloys, the transformation entropy changes evolve during aging. Figure 6 shows the evolution of the average absolute value of the entropy change (ΔS) *versus* aging time at 470 K, after water quench from 970 K, for alloys C2 (a) and C4 (b). In both cases the transformation entropy decreases with increasing aging time, again recalling the well-known relationship between ΔS and ($T_C^A - T_O$). Aside from this general trend, it can be observed that, for alloy C2, ΔS shows no changes while the $A_{para}\leftrightarrow m_{para}$ occurs, decreases when it switches to $A_{ferro}\leftrightarrow m_{para}$ and remains constant when all transformation temperatures are stable. For alloy C4, ΔS is constant while the $A_{ferro}\leftrightarrow m_{para}$ takes place and the transformation temperatures are constant, and changes start when the $A_{ferro}\leftrightarrow m_{ferro}$ transition shows up. The ΔS evolution shows an inflection giving way to a slight increase when the swap is complete

Figure 6. Evolution of the transformation entropy (average absolute values, ΔS) as a function of post-quench aging time at 470 K for alloys C2 (a) and C4 (b) (adapted from [15]).

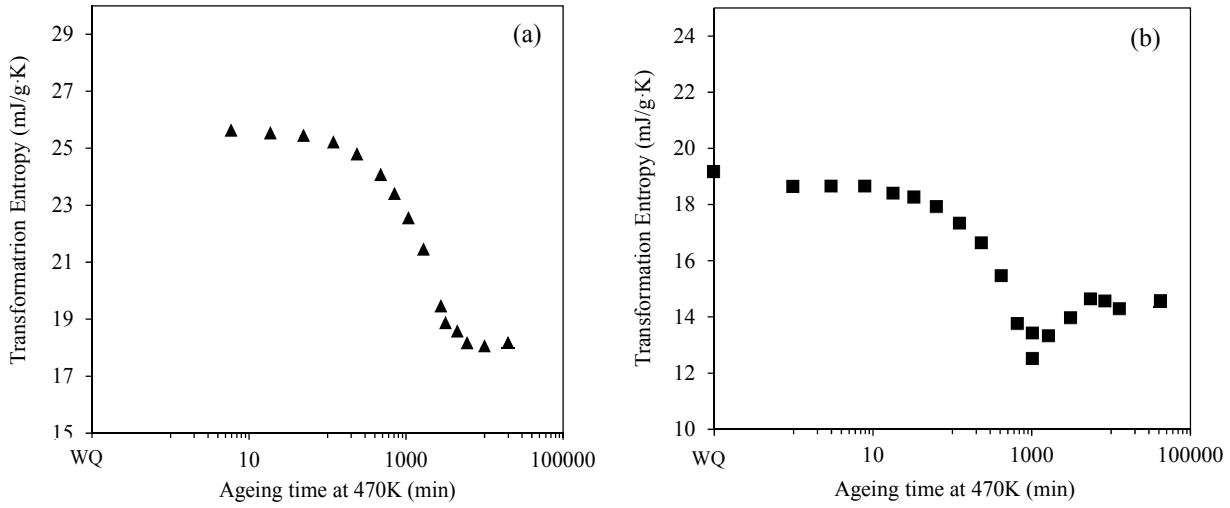

3.5. Quantitative Evaluation of the Magnetic Entropy

In the above sections the dependence of ΔS on composition and atomic ordering has been shown and analyzed basing on the relationship between the magnetic contribution to the transformation entropy and the temperature gap ($T_C^A - T_O$).

Beyond the qualitative agreement, for $A_{ferro}\leftrightarrow m_{para}$ MT, between increasing ($T_C^A - T_O$) and increasing ΔS_{mag}, the actual, specific, relationship between ($T_C^A - T_O$) and ΔS_{mag}, the way how switching of the magnetic exchange across the MT affects ΔS_{mag} and the quantitative evaluation of the magnetic contribution are not directly inferred from the results.

Recently, a model based on the Bragg-Williams mean-field approach has been developed to account for ΔS_{mag}, which has been successfully tested with the experimental data obtained from different metamagnetic alloys displaying either $A_{ferro} \leftrightarrow m_{para}$ or $A_{ferro} \leftrightarrow m_{ferro}$ MTs [27]. The model has also been applied to the present alloys belonging to the Ni-Co-Mn-Ga system, with different degrees of atomic order, resulting in a very good agreement between experimental values of the transformation entropy and those predicted by the theory [27]. In the frame of the model, the entropy associated to a given value of an order parameter m is:

$$S(m) = k_B \left\{ ln\,2 - \frac{1}{2}(1+m)ln(1+m) - \frac{1}{2}(1-m)ln(1-m) \right\} \tag{7}$$

To obtain the magnetic entropy associated to a given magnetic order, the reduced spontaneous magnetization $m = M(T)/M(0)$ is taken as order parameter, so that for austenite (A) and martensite (m) we have:

$$S_{mag}^{A} = k_B \left\{ \ln 2 - \frac{1}{2}(1+m_A)\ln(1+m_A) - \frac{1}{2}(1-m_A)\ln(1-m_A) \right\} \tag{8}$$

$$S_{mag}^{m} = k_B \left\{ \ln 2 - \frac{1}{2}(1+m_m)\ln(1+m_m) - \frac{1}{2}(1-m_m)\ln(1-m_m) \right\} \tag{9}$$

where m_A, m_m are the reduced spontaneous magnetization of austenite and martensite, respectively; the magnetic entropy change in the forward MT is then

$$\Delta S_{mag}^{A\to m} = \Delta S_{mag}^{m} - \Delta S_{mag}^{A} = \frac{k_B}{2}\left\{ \left[(1+m_A)\ln(1+m_A) + (1-m_A)\ln(1-m_A) \right] - \left[(1+m_m)\ln(1+m_m) + (1-m_m)\ln(1-m_m) \right] \right\} \tag{10}$$

Since the spontaneous magnetization curves for the studied alloys are not available, m_A and m_m will be calculated with the help of the expression obtained by Kuz'min for the temperature dependence of the spontaneous magnetization of ferromagnets [31], resulting in:

$$m_A = \frac{M_A(T)}{M_A(0)} = \left[1 - s(1-\delta_A)^{\frac{3}{2}} - (1-s)(1-\delta_A)^{\frac{5}{2}} \right]^{\frac{1}{3}} \tag{11}$$

$$m_m = \frac{M_m(T)}{M_m(0)} = \left[1 - s(1-\delta_m)^{\frac{3}{2}} - (1-s)(1-\delta_m)^{\frac{5}{2}} \right]^{\frac{1}{3}} \tag{12}$$

Here δ_A, δ_m are the reduced temperature differences $\delta_A(T) = \left(T_C^A - T\right)/T_C^A$ and $\delta_m(T) = \left(T_C^m - T\right)/T_C^m$, and s is a parameter related to the shape of the magnetization curves, taken as s=0.1 for austenite and s = 2.2 for martensite. Obviously, when the $A_{para} \leftrightarrow m_{para}$ occurs $m_A = m_m = 0$ and $\Delta S_{mag} = 0$, whereas $m_A \neq 0$, $m_m = 0$, hence $\Delta S_{mag} > 0$ for the $A_{ferro} \leftrightarrow m_{para}$ transition and $m_A \neq 0$, $m_m \neq 0$, so $\Delta S_{mag} > 0$ or $\Delta S_{mag} < 0$ for the $A_{ferro} \leftrightarrow m_{ferro}$ MT.

Figure 7. Experimental (absolute values: □ alloy C2, ● alloy C4) and calculated magnetic entropy (dashed lines and ∗, ∗ for $A_{ferro}\leftrightarrow m_{para}$, ∗ for $A_{ferro}\leftrightarrow m_{ferro}$ MTs) as a function of the reduced temperature difference at the transformation temperature $\delta_A(T_O)$. The structural contribution has been chosen as $\Delta S_{strc} = 26\ J\cdot kg^{-1}\cdot K^{-1}$.

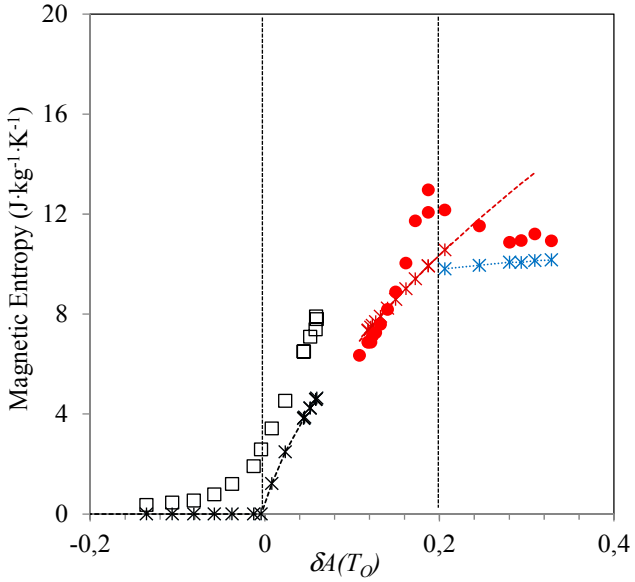

The described model has been successfully applied to the data obtained for alloys C1 to C5 subjected to different thermal treatments. As an example, Figure 7 shows the calculated and experimental magnetic entropy changes for alloys C2 and C4 along post-quench ageing as a function of $\delta_A(T_O)$. On the one hand, for each ageing time, the reduced transformation temperatures $\delta_A(T_o)=\left(T_C^A - T_o\right)/T_C^A$ and $\delta_m(T_o)=\left(T_C^m - T_o\right)/T_C^m$ allow obtaining the reduced spontaneous magnetization of the phases m_A and m_m from which ΔS_{mag} is calculated. The transformation and Curie temperatures are those shown in Figure 3. On the other hand, the magnetic contribution to the measured transformation entropy values shown in Figure 5 is evaluated as $\Delta S_{mag} = \Delta S_{strc} - \Delta S$. The structural contribution has been chosen as $\Delta S_{strc} = 26\ J\cdot kg^{-1}\cdot K^{-1}$, corresponding to the $A_{para}\leftrightarrow m_{para}$ MT undergone by alloy C2 after quench. Figure 7 shows excellent fitting of the model to the experimental ΔS_{mag}. It is worth to mention that, besides the change from $A_{para}\leftrightarrow m_{para}$ to $A_{ferro}\leftrightarrow m_{para}$ obviously taking place at $\delta_A(T_O) = 0$, switch from $A_{ferro}\leftrightarrow m_{para}$ to $A_{ferro}\leftrightarrow m_{ferro}$ occurs at $\delta_A(T_O) \approx 0.2$, in agreement with published results obtained for other alloy systems [27]. The magnetic origin of the stages observed in Figure 5 is also validated by the model, strengthening its validity regardless of the alloy composition and atomic order condition.

According to Figure 7 the magnetic contribution to the transformation entropy can be quantitatively evaluated quite rigorously in relation to $\left(T_C^A - T_o\right)/T_C^A$. For the studied alloys, the maximum value of the magnetic entropy amounts 10–12 $J\cdot kg^{-1}\cdot K^{-1}$ and corresponds to the switch from $A_{ferro}\leftrightarrow m_{para}$ to $A_{ferro}\leftrightarrow m_{ferro}$, as already discussed in 3.3 section. Being about 40% of the structural contribution to the transformation entropy, for the present alloy system the emergence of $A_{ferro}\leftrightarrow m_{ferro}$ MT prevents the magnetic entropy from growing enough as to counterbalance the structural contribution leading to thermodynamic arrest of the MT.

4. Conclusions

The transformation entropy change (ΔS) accompanying the magnetostructural transformation undergone by $Ni_{50-x}Co_xMn_{25+y}Ga_{25-y}$ (x = 3–8, y = 5–7) alloys has been analyzed. For these alloys, combined composition and thermal treatment allows obtaining different magnetic exchanges across the MT –*i.e.*, $A_{para}\leftrightarrow m_{para}$, $A_{ferro}\leftrightarrow m_{para}$ or $A_{ferro}\leftrightarrow m_{ferro}$–. Such behavior is due to the modification of L21 order degree by means of thermal treatments, which produces transformation temperature changes resulting in variation of the transformation sequence. Consequently, both the magnetization jump across the MT (ΔM) and ΔS are composition and atomic order dependent.

For a magnetostructural transition ΔS comprises structural and magnetic contributions, the latter being considered as the main responsible for the observed changes. The key results regarding the behavior of the transformation entropy in relation to composition and atomic order in the Ni-Co-Mn-Ga alloy system are summarized as follows:

(1) $\Delta S_{mag}^{A\to m}=0$ if neither austenite nor martensite exhibit magnetic order, as in a $A_{para}\leftrightarrow m_{para}$ transformation; instead, $\Delta S_{mag}^{A\to m}>0$ (and $\Delta S_{mag}^{m\to A}<0$) in a metamagnetic $A_{ferro}\leftrightarrow m_{para}$ MT. For a $A_{ferro}\leftrightarrow m_{ferro}$ MT, $\Delta S_{mag}^{A\to m}$ can be either positive or negative depending on the relative value of magnetization of austenite and martensite. For metamagnetic MTs, $|\Delta S_{mag}|$ increases with increasing ($T_C^A - T_O$), hence the overall ΔS diminishes. However, owing to the thermal hysteresis of the MT, ($T_C^A - M_p$) > ($T_C^A - A_p$), so in general $\left|\Delta S_{mag}^{A\to m}\right|>\left|\Delta S_{mag}^{m\to A}\right|$ and $|\Delta S^{A\to m}|<|\Delta S^{m\to A}|$.

(2) The transformation entropy increases towards higher *e/a* values, for which ($T_C^A - T_O$) decreases; for low *e/a*, the MT changes from $A_{ferro}\leftrightarrow m_{para}$ to $A_{ferro}\leftrightarrow m_{ferro}$ for which ΔM is smaller, the corresponding ΔS_{mag} decreases and thus the (absolute value) overall transformation entropy increases. In any case, ΔS_{mag} is the highest for the *e/a* values for which the MT switches from $A_{ferro}\leftrightarrow m_{para}$ to $A_{ferro}\leftrightarrow m_{ferro}$, where decrease triggered by the increasingly ferromagnetic martensite starts.

(3) ΔS reflects the changes of atomic order degree produced by thermal treatments, again recalling the relationship between ΔS and ($T_C^A - T_O$). The evolution of ΔS as a function of post-quench ageing time shows different stages related to the occurrence of the $A_{para}\leftrightarrow m_{para}$, $A_{ferro}\leftrightarrow m_{para}$ and $A_{ferro}\leftrightarrow m_{ferro}$ transitions.

(4) The magnetic contribution to the transformation entropy can be quantitatively evaluated by means a phenomenological model which has been recently developed, based on a Bragg–Williams approximation. The model provides an expression for ΔS_{mag} as a function of the reduced temperature differences $\left(T_C^A - T\right)/T_C^A$ and $\left(T_C^m - T\right)/T_C^m$, and has been applied to the data obtained for $Ni_{50-x}Co_xMn_{25+y}Ga_{25-y}$ (x = 3–8, y = 5–7) alloys subjected to different thermal treatments. Excellent fitting between the calculated and the experimental values of ΔS_{mag} is obtained, including the switching from one transformation sequence to another. In this way, the magnetic origin of the stages observed in the ΔS *vs* ageing time evolution is also validated by the model, strengthening its validity regardless of the alloy composition and atomic order condition.

(5) For the studied Ni-Co-Mn-Ga alloys, the maximum value of the magnetic entropy change amounts to 10–12 $J\cdot kg^{-1}\cdot K^{-1}$ (about 40% of the structural contribution) and corresponds to the switch from $A_{ferro}\leftrightarrow m_{para}$ to $A_{ferro}\leftrightarrow m_{ferro}$.

Acknowledgments

Partial financial support from MINECO and FEDER (project MAT 2011-28217-C02-01) is acknowledged.

Author Contributions

Concepció Seguí performed most the experimental work. Eduard Cesari was responsible for the application of the Bragg-Williams model to the transformation entropy and provided important inputs on the scientific analysis of the results. Both authors contributed equally to the writing and have read and approved the final manuscript

Conflicts of Interest

The authors declare no conflict of interest.

References

1. Sutou, Y.; Imano, Y.; Koeda, N.; Omori, T.; Kainuma, R.; Ishida, K.; Oikawa, K. Magnetic and martensitic transformations of NiMnX (X=In, Sn, Sb) ferromagnetic shape memory alloy. *Appl. Phys. Lett.* **2004**, *85*, 4358–4360.
2. Kainuma, R.; Imano, Y.; Ito, W; Morito, H.; Sutou, Y.; Oikawa, K.; Fujita, A.; Ishida, K.; Okamoto, S.; Kitakami, O.; Kanomata, T. Metamagnetic shape memory effect in a Heusler-type $Ni_{43}Co_7Mn_{39}Sn_{11}$ polycrystalline alloy. *Appl. Phys. Lett.* **2006**, *88*, 192513.
3. Yu, S.Y.; Cao, Z.X.; Ma, L.; Liu, G.D.; Chen, J.L.; Wu, G.H.; Zhang, B.; Zhang, X.X. Realization of magnetic field induced reversible martensitic transformation in NiCoMnGa alloys. *Appl. Phys. Lett.* **2007**, *91*, 102507.
4. Oikawa, K.; Ito, W.; Imano, Y.; Sutou, Y.; Kainuma, R.; Ishida, K.; Okamoto, S.; Kitakami, O.; Kanomata, T. Effect of magnetic field on martensitic transition of $Ni_{46}Mn_{41}In_{13}$ Heusler alloy. *Appl. Phys. Lett.* **2006**, *88*, 122507.
5. Koyama, K.; Watanabe, K.; Kanomata, T.; Kainuma, R.; Oikawa, K.; Ishida, K. Observation of field-induced reverse transformation in ferromagnetic shape memory alloy $Ni_{50}Mn_{36}Sn_{14}$. *Appl. Phys. Lett.* **2006**, *88*, 132505.
6. Krenke, T.; Duman, E.; Acet, M.; Wassermann, E.F.; Moya, X.; Mañosa, L.; Planes, A. Inverse magnetocaloric effect in ferromagnetic Ni-Mn-Sn alloys. *Nat. Mater*. **2005**, *4*, 450–454.
7. Sharma, V.K.; Chattopadhyay, M.K.; Shaeb, K.H.B.; Chouhan, A.; Roy, S.B. Large magnetoresistance in $Ni_{50}Mn_{34}In_{16}$ alloy. *Appl. Phys. Lett.* **2006**, *89*, 222509.
8. Kainuma, R.; Imano, Y.; Ito, W.; Sutou, Y.; Morito, H.; Okamato, H.; Kitakami, S.; Oikawa, O.; Fujita, A.; Kanomata, T. Magnetic-field-induced shape recovery by reverse phase transformation. *Nature* **2006**, *439*, 957–960.
9. Yu, S.Y.; Ma, L.; Liu, G.D.; Liu, Z.H.; Chen, J.L.; Cao, Z.X.; Wu, G.H.; Zhang, B.; Zhang, X.X. Magnetic field-induced martensitic transformation and large magnetoresistance in NiCoMnSb. *Appl. Phys. Lett.* **2007**, *90*, 242501.

10. Khovailo, V.V.; Novosad, V.; Takagi, T.; Filippov, D.A.; Levitin, R.Z.; Vasil'ev, A.N. Magnetic properties and magnetostructural phase transitions in $Ni_{2+x}Mn_{1-x}Ga$ shape memory alloys. *Phys. Rev. B* **2004**, *70*, 174413.
11. Sánchez-Alarcos, V.; Pérez-Landazábal, J.I.; Recarte, V.; Gómez-Polo, C.; Rodríguez-Velamazán, J.A. Correlation between composition and phase transformation temperatures in Ni-Mn-Ga-Co ferromagnetic shape memory alloys. *Acta Mater.* **2008**, *56*, 5370–5376.
12. Fabbrici, S.; Albertini, F.; Paoluzi, A.; Bolzoni, F.; Cabassi, R.; Solzi, M.; Righi, L.; Calestani, G. Reverse magnetostructural transformation in Co-doped NiMnGa multifunctional alloys. *Appl. Phys. Lett.* **2009**, *95*, 022508.
13. Fabbrici, S.; Kamarad, J.; Arnold, Z.; Casoli, F.; Paoluzi, A.; Bolzoni, F.; Cabassi, R.; Solzi, M.; Porcari, G.; Pernechele, C.; *et al.* From direct to inverse giant magnetocaloric effect in Co-doped NiMnGa multifunctional alloys. *Acta Mater.* **2011**, *59*, 412–419.
14. Seguí, C.; Cesari, E. Effect of ageing on the structural and magnetic transformations and the related entropy change in a Ni-Co-Mn-Ga ferromagnetic shape memory alloy. *Intermetallics* **2011**, *19*, 721–725.
15. Seguí C.; Cesari E. Composition and atomic order effects on the structural and magnetic transformations in ferromagnetic Ni-Co-Mn-Ga shape memory alloys. *J. Appl. Phys.* **2012**, *111*, 043914.
16. Sakon, T.; Sasaki, K.; Numakura, D.; Abe, M.; Nojiri, H.; Adachi, Y.; Kanomata, T. Magnetic field-induced transition in Co-doped $Ni_{41}Co_9Mn_{31.5}Ga_{18.5}$ Heusler alloy. *Mater. Trans.* **2013**, *54*, 9–13.
17. Xu, X.; Ito, W.; Umetsu, R.Y.; Koyama, K.; Kainuma, R.; Ishida, K. Kinetic arrest of martensitic transformation in $Ni_{33.0}Co_{13.4}Mn_{39.7}Ga_{13.9}$ metamagnetic shape memory alloy. *Mater. Trans.* **2010**, *51*, 469–471.
18. Sánchez-Alarcos, V.; Pérez-Landazábal, J.I.; Recarte, V.; Cuello, G.J. Correlation between atomic order and the characteristics of the structural and magnetic transformations in Ni-Mn-Ga shape memory alloys. *Acta Mater.* **2007**, *55*, 3883–3889.
19. Chernenko, V.A.; Cesari, E.; Pons, J.; Seguí, C. Phase Transformations in Rapidly Quenched Ni-Mn-Ga Alloys. *J. Mater. Res.* **2000**, *15*, 1496–1504.
20. Seguí, C.; Pons, J.; Cesari, E. Effect of atomic ordering on the phase transformations in Ni-Mn-Ga shape memory alloys. *Acta Mater.* **2007**, *55*, 1649–1655.
21. Sanchez-Alarcos, V.; Recarte, V.; Pérez-Landazabal, J.I.; Gómez-Polo, C.; Rodríguez-Velamazán, J.A. Role of magnetism on the martensitic transformation in Ni-Mn-based magnetic shape memory alloys. *Acta Mater.* **2012**, *60*, 459–468.
22. Recarte, V.; Pérez-Landazábal, J.I.; Sánchez-Alarcos, V.; Rodríguez-Velamazán, J.A. Dependence of the martensitic transformation and magnetic transition on the atomic order in Ni-Mn-In Metamagnetic Shape Memory Alloys. *Acta Mater.* **2012**, *60*, 1937–1945.
23. Seguí, C. Effects of the interplay between atomic and magnetic order on the properties of metamagnetic Ni-Co-Mn-Ga shape memory alloys. *J. Appl. Phys.* **2014**, *115*, 113903.
24. Khovaylo, V.V.; Oikawa, K.; Abe, T.; Tagaki, T. Entropy change at the martensitic transformation in ferromagnetic shape memory alloys $Ni_{2+x}Mn_{1-x}Ga$. *J. Appl. Phys.* **2003**, *93*, 8483–8485.

25. Ito, W.; Imano, Y.; Kainuma, R.; Sutou, Y.; Oikawa, K.; Ishida, K. Martensitic and magnetic transformation behaviors in Heusler-type NiMnIn and NiCoMnIn metamagnetic shape memory alloys. *Metall. Mater. Trans.* **2007**, *38*, 759–766.
26. Kustov, S.; Corró, M.L.; Pons, J.; Cesari, E. Entropy change and effect of magnetic field on martensitic transformation in a metamagnetic Ni-Co-Mn-In shape memory alloy. *Appl. Phys. Lett.* **2009**, *94*, 191901.
27. Recarte, V.; Pérez-Landazábal, J.I.; Sánchez-Alarcos, V.; Zablotskii, V.; Cesari, E.; Kustov, S. Entropy change linked to the martensitic transformation in metamagnetic shape memory alloys. *Acta. Mater.* **2012**, *60*, 3168–3175.
28. Wang, B.M.; Ren, P.; Liu, Y.; Wang, L. Enhanced magnetoresistance through magnetic-field-induced phase transition in Ni_2MnGa co-doped with Co and Mn. *J. Mag. Mat.* **2010**, *322*, 715–717.
29. Ito, V.; Nagasako, R.; Umetsu, R.Y.; Kainuma, R.; Kanomata, T.; Ishida, K. Atomic ordering and magnetic properties in the $Ni_{45}Co_5Mn_{36.7}In_{13.3}$ metamagnetic shape memory alloy. *Appl. Phys. Lett.* **2008**, *93*, 232503.
30. Barandiarán, J.M.; Chernenko, V.A.; Cesari, E.; Salas, D.; Gutiérrez, J.; Lazpita, P. Magnetic field and atomic order effect on the martensitic transformation of a metamagnetic alloy. *J. Phys. Condens. Matter* **2013**, *25*, 484005.
31. Kuz'min, M.D. Shape of temperature dependence of spontaneous magnetization of ferromagnets: Quantitative analysis. *Phys. Rev. Lett*. **2005**, *94*, 107204.